

Power harvesting in a helicopter lag damper

P. H. de Jong MSc., R. Loendersloot, A. de Boer, P. J. M. van der Hoogt
Structural Dynamics & Acoustics group, University of Twente, Enschede, the Netherlands

ABSTRACT: In this paper a new power harvesting application is developed and simulated. Power harvesting is chosen within the European Clean Sky project as a solution to powering in-blade health monitoring systems as opposed to installing an elaborate electrical infrastructure to draw power from and transmit signals to the helicopter body. Local generation of power will allow for a ‘plug and play’ rotor blade and signals may be logged or transmitted wirelessly.

The lag damper is chosen to be modified as it provides a well defined loading due to the regressive damping characteristic. A piezo electric stack is installed inside the damper rod, effectively coupled in series with the damper. Due to the well defined peak force generated in the damper the stack geometry requires a very limited margin of safety. Typically the stack geometry must be chosen to prevent excessive voltage build-up as opposed to mechanical overload.

Development and simulation of the model is described starting with a simplified blade and piezo element model. Presuming specific flight conditions transient simulations are conducted using various power harvesting circuits and their performance is evaluated. The best performing circuit is further optimized to increase the specific power output. Optimization of the electrical and mechanical domains must be done simultaneously due to the high electro-mechanical coupling of the piezo stack. The non-linear electrical properties of the piezo material, most notably the capacitance which may have a large influence, are not yet considered in this study.

The power harvesting lag damper provides sufficient power for extensive health monitoring systems within the blade while retaining the functionality and safety of the standard component. For the 8.15m blade radius and 130 knots flight speed under consideration simulations show 7.5 watts of power is generated from a single damper.

1 INTRODUCTION

Power harvesting devices using piezo electric materials typically focus on a limited number of applications: base excited resonant beams and elastically deforming structures augmented with a small patch. A number of specific applications have been investigated as well, ranging from custom shapes (e.g.: cymbals, (Dogan, Fernandez, et. al., 1996)) to special applications (helicopter pitch rods (Arms, Townsend, et. al., 2006), backpack straps (Feenstra, Granstorm, Sodano, 2008)). The bulk of the research focuses on benders due to their intrinsic stress amplification on the piezo electric material using a limited base excitation. The topics cover basic shape variation (Dietl, Garcia, 2010), geometry optimization (Zheng et.al., 2009) and increasing the bandwidth of a system (Wickenheiser, Garcia, 2010). Stacks are rarely used as they require large forces to produce a useful charge (Anton, Sodano, 2006), precisely the loading which is present in a lag damper.

On the electronics side, a considerable amount of research has been done towards optimal circuits which boost the power output. Examples include the 3 following similar techniques of voltage biasing (Dicken et. al., 2009), feeding energy back in to the patch to increase output (Shen et.al., 2010) and the Synchronized Switch Harvesting on Inductor (SSHI) circuit (Guyomar et.al., 2005), and other active circuits such as Synchronized Electric Charge Extraction (SECE) (Lefeuvre et.al., 2005). However, a complete power harvesting solution spanning from material choice and application to circuit consideration is rarely presented.

A small amount of research has also been done towards the effects of varying electromechanical coupling but only in resonant conditions [7,8]. The application of more efficient circuits allows for less piezoelectric material and a lower coupling. In non-resonant devices only the relatively inefficient impedance matching technique has been applied (Feenstra et.al., 2008) whereas the aforementioned more advanced circuits are far more capable under these circumstances (Lefeuvre et.al., 2006). Using the same amount of material up to a tenfold increase in output may be achieved for non-resonant systems.

Here a power harvesting device is presented in which material choice and construction is considered as well as the choice of circuit. The envisaged application is within a helicopter lag damper: a device which dampens in-plane blade oscillations on rotor craft in order to suppress air and ground resonance. The concept is also unique in that it utilizes a directly excited stack which is possible due to the high 9kN force available (Maybury et.al., 2009). A drawback of these circuits when used in sub-resonant systems is the mechanical oscillations resulting from the harvesting circuit rapidly changing the stack voltage. In this case however they are damped out due to the very high damping of the mechanical system.

Firstly, piezo electric materials are compared on a mechanical and electrical basis to determine the best type. Secondly a power harvesting circuit is chosen for use. Following analytical considerations the chosen circuit is further investigated and optimized for the concept and an output is determined. Phenomena not considered in this paper are temperature effects and non-linear capacitance of the piezoelectric material (Yang et.al., 2008). Both have a notable negative influence on the performance.

The final goal is to establish how much power can be harvested from such a lag damper system. This power can be used to power for example local health monitoring systems. It is difficult to power these systems by drawing electricity from the body of the helicopter since it requires extensive infrastructure around the rotor shaft to transport electricity and measurement signals. Monitoring the condition of the blades will allow them to be replaced when the blades have reached the end of their lifespan as opposed to replacing uninstrumented blades based on a very conservative lifetime calculation. Some developing technologies focus on impact damage events such as bird or munitions strikes alerting the pilot to critical damage.

2 MODELLING

The lag damper is designed to suppress air- and ground-resonance. These phenomena result from the coupling of aerodynamics and structure dynamics. Since this energy is otherwise dissipated as heat it provides an efficient excitation.

The lag damper is taken from a rotor with an 8.15m radius. The flight configuration under consideration is straight and level flight, with a velocity of 130 knots (66.9m/s). Due to changes in relative airspeed over the blades on the left and right side of the rotorcraft, the blade pitch must also be varied via pilot control. This leads to cyclic variations of drag and lift as the blade performs one revolution (Bramwell, 2001). The developed damper force F_0 resembles a step function with a 9kN amplitude with a frequency identical to that of the rotor speed Ω of 4.18Hz. The rotor speed is the dominant frequency that the damper is subjected to. The force F_0 is a built-in limit in the damper and is reached during forward flight, presenting a consistent and prevalent excitation. A design outline is shown in Figure 1 and the force-velocity profile is given in Figure 2.

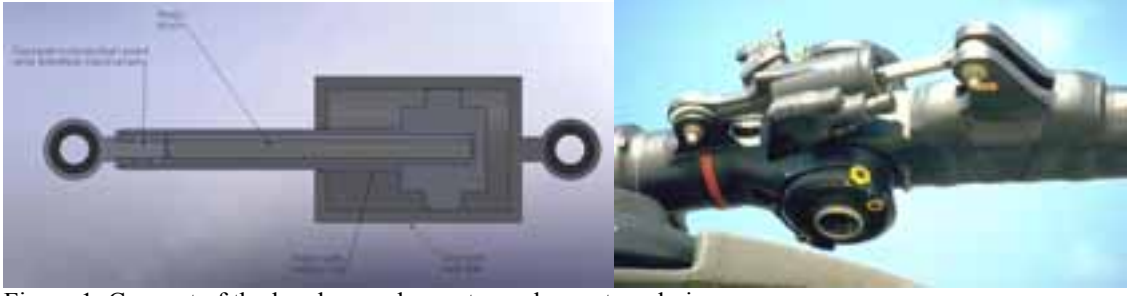


Figure 1: Concept of the lag damper harvester and an external view

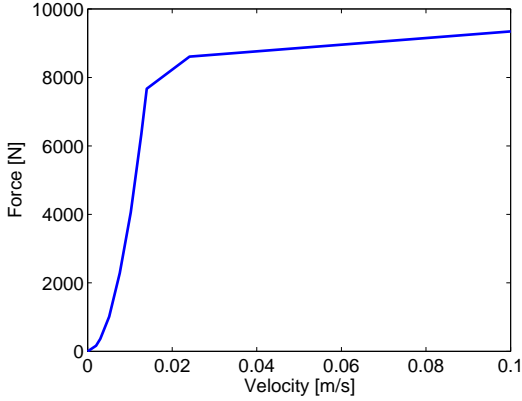


Figure 2: Lag damper force-velocity profile

2.1 Materials

For material selection two aspects are important: piezoelectric performance and reverse voltage bias. Low permittivity is also advantageous as it decreases reactive power in the circuit. Most properties are summarized in the coupling coefficient k , indicating how well a material converts mechanical strain to electrical energy. When considering materials by PICeramics for example, only 4 materials are categorized as ‘hard’ PZT implying high electromechanical stability and relatively high resistance to depolarization. PIC300 and PIC181 have the highest Curie temperature and coupling respectively. Considering the application of rotorcraft where a maximum of 70 degrees is specified the choice falls upon PIC181 with its far superior coupling. Further material data is given in Table 1.

Table 1: Material data PIC181 (source: PI Ceramic)

Density ρ	7800 kg/m ³
Youngs modulus (1D stress, 33 direction) E_{33}	71 GPa
Piezo electric coefficient e_{33}	14.7 N/Vm
Relative permittivity ϵ_r^σ	1200 -
Maximum stress σ_{max}	120 MPa
Maximum reverse bias field E_v (room temp)	10 ⁶ V/m
Curie Temperature	330 °C
Coupling k_{33}	0.66 -

Based on the maximum material stress the cross section can be determined as $1.5 \cdot 10^{-4} \text{m}^2$. This is based on a compressive force of 18kN, twice the amplitude of the lag damper due to the stack being pre-stressed to 9kN. From this the short circuit stiffness k_p and capacitance C_p of the stack are calculated as:

$$k_p = \frac{E_{33}A}{L}, \quad C_p = \frac{\epsilon^\sigma nA}{t_l} \quad (1)$$

With n representing the number of layers in the stack. The layer thickness t_l will later be varied to investigate any influences on the performance of the circuit.

2.2 Mechanical model

Using data provided by *AgustaWestland Helicopters (AW)* it can be determined that a 1 degree of freedom (DOF) model is acceptable for the blade. Figure 3 shows results from *AW* simulations and the 1DOF blade model. The damper velocity matches reasonably well but the insensitivity of the force above 0.02m/s allows for an acceptable approximation.

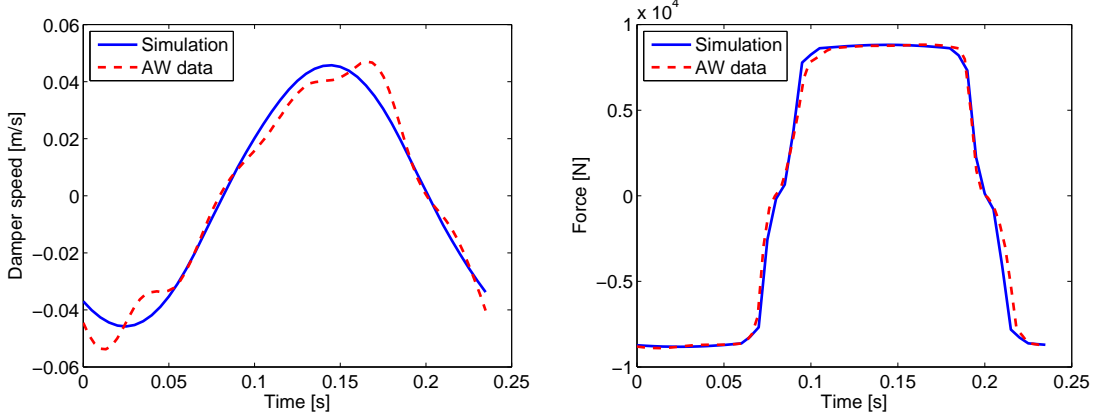


Figure 3: Damper velocity and force for 1DOF blade model. AW data (red dashed) and 1DOF simulation (blue solid)

The stack also possesses one DOF representing the displacement. The damper and stack are in series and the excitation of the stack is generated by the velocity change in the damper. A 2DOF model for power harvesting is shown in Figure 4. It shows the blade represented by 1 DOF with moment of inertia J , excitation moment M_0 , an equivalent rotary spring k_{eq} to represent the centrifugal stiffening effect at constant rotor speed, the lag damper, piezo electric stack with DOF u and a mass M representing the piston. The moment is chosen such that the model and *AW* data yield the same amount of dissipated energy.

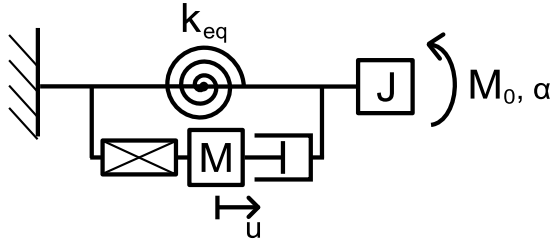


Figure 4: Blade and stack IPM

For the stack the maximum permissible dimensions within the damper rod are 20mm in diameter and 0.25m in length. A shorter stack is of course possible but for the sake of determining the maximum achievable output the largest dimensions are assumed.

2.3 Electrical model

The piezo electric element is modeled using the following equations:

$$\begin{aligned} k_p u(t) + \theta V(t) &= F(t) \\ \theta \dot{u}(t) - C_p \dot{V}(t) &= I(t) \end{aligned} \quad , \quad \theta = \frac{e_{33} A}{t_l} \quad (2)$$

With V representing the voltage, $F(t)$ the external force and θ the electromechanical coupling. The Synchronized Switch Harvesting on Inductor (SSHI) circuit (Guyomar et.al., 2005) is used

to extract the electrical energy from the stack. The DC Impedance matching (Shu et.al, 2006) and Synchronous Electric Charge Extraction circuit (Lefeuvre et.al., 2005) were briefly investigated as well but did not perform as well. Based on (Lefeuvre et.al., 2006) the use of the SSHI circuit in a non-resonant system allows for a significant increase in output over other circuits. SSHI utilizes a switched inductor coupled with the stack capacitance to create an electrical oscillator. Upon displacement extrema the inductor is switched on for half of one period allowing the voltage to change polarity. This inversion must happen sufficiently quick to avoid a significant change in force on the stack. The displacement and voltage waveforms are given in Figure 5. The current is conducted away from the piezo element via a diode rectifier to a storage circuit.

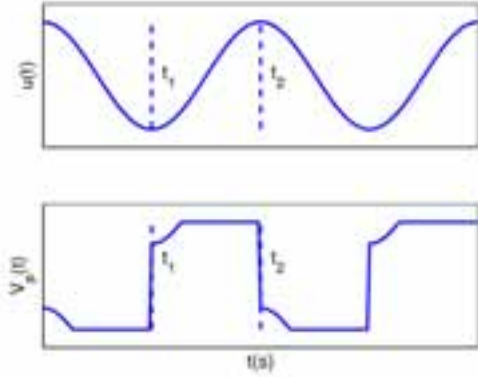


Figure 5: SSHI displacement and voltage waveforms

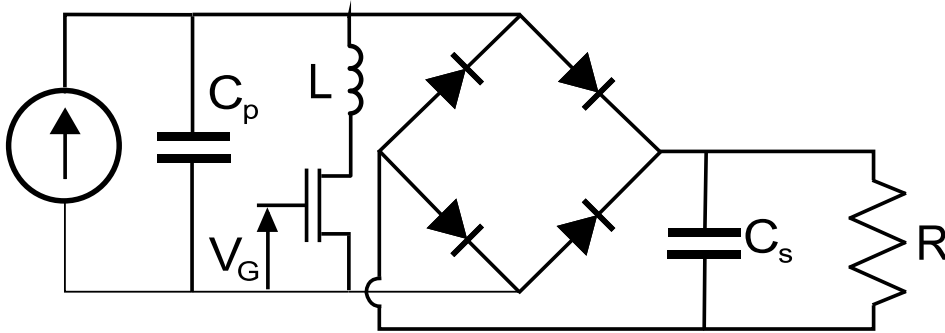


Figure 6: SSHI electrical schematic

Figure 6 shows the circuit with the piezo element (current generator and capacitance C_p), the switched inductor L , the diode rectifier, storage capacitance C_s and resistive load R . The inductor adds a parasitic resistance which is accounted for using the inductor quality Q_i . A higher value of Q_i indicates lower electrical losses. Similar to the DC impedance matching circuit the SSHI circuit possesses an optimal resistance value (Shu et.al., 2007), written as:

$$R_{opt} = \frac{\pi}{C_p \left(1 - e^{\frac{-\pi}{2Q_i}} \right) \omega} \quad (3)$$

Due to the high stress imposed on the material this optimum resistance will drive the voltage up beyond the maximum reverse bias. Rewriting equation (20) from (Shu et.al., 2007) and assuming a low frequency excitation compared to the mechanical natural frequency ($\Omega \ll \omega_{mech}$) the following equation is found yielding the maximum resistance R as a function of the maximum voltage field $V_{p,max}$, excitation force F_0 and stack properties k_p , C_p and θ :

$$R = \frac{\pi V_{p,\max} k_p}{\Omega \left(\left[2F_0 - V_{p,\max} \left(1 - e^{\frac{-\pi}{2Q_i}} \right) \right] \theta - k_p C_p V_{p,\max} \left(1 - e^{\frac{-\pi}{2Q_i}} \right) \right)} \quad (4)$$

Another issue concerns the capacitor-inductor oscillator. For low coupled systems the inversion duration adheres to that of the electrical domain only. Here the high coupling implies that the full electromechanical equations must be solved to find the optimum inversion duration. Moreover the very high damping resulting from the lag damper ($\zeta=0.75$) must be taken into account. For the inversion process alone a linear system can be assumed. Note that operation of the damper is also assumed linear, implying the velocity remains above 0.02m/s as according to Figure 2. The damping coefficient for the final linear portion above 0.02m/s is $C=9700\text{Ns/m}$. Solving the 3DOF system (blade angle α , stack displacement u and voltage V) is not necessary as the inertia of the blade is sufficiently high to ignore the influence of the blade motion. The following 2DOF equation (u and V) is solved yielding the natural frequency ω_{em} of the electro-mechanical oscillation:

$$\begin{bmatrix} M & 0 \\ 0 & C_p \end{bmatrix} \ddot{q} + \begin{bmatrix} C & \theta \\ -\theta & R_L \end{bmatrix} \dot{q} + \begin{bmatrix} k_p & 0 \\ 0 & \frac{1}{L} \end{bmatrix} q = 0, \quad \dot{q} = \begin{Bmatrix} \dot{u} \\ V \end{Bmatrix} \quad (5)$$

Lastly the inversion duration influences the efficiency of inversion. As indicated the high electromechanical coupling implies a response in the damped mechanical domain. Minimizing viscous losses requires as slow inversion as possible to reduce the velocity \dot{u}^2 , as demonstrated in Figure 7. The horizontal axis shows the time normalized with the period of the oscillation and the vertical axis the normalized voltage. The solid line represents very quick inversion ($\omega_{em} \gg \omega_{mech}$) where initially the efficiency is better but as the mechanical domain is excited and settles towards the new equilibrium a significant amount of energy is lost. The dashed line represents very slow inversion ($\omega_{em} \ll \omega_{mech}$) where the electromechanical frequency is chosen much lower than that of the mechanical domain. The mechanical DOF follows immediately and slowly minimizing viscous losses.

Summarizing the inversion time the circuit requires quick inversion to prevent any significant change in the applied force which would lead to losses in harvested power. On the other hand the inversion must not be too quick due to the highly damped mechanical domain.

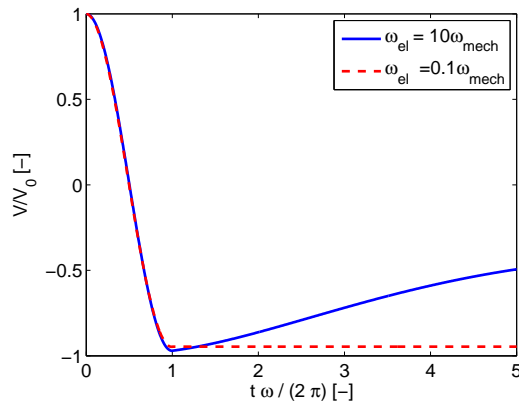


Figure 7: Voltage inversion efficiency vs frequency, fast (solid) and slow (dashed) inversion

3 RESULTS

A MATLAB / Simulink / Simscape model is made according to the model described in section 2. The optimal parameters for the model as given in Table 2 are used. The simulation is run for 100 rotor rotations after which a quasi-static state has been achieved. Figure 8 and Figure 9 give results for a single simulation, showing the dissipated power starting from a discharged state and the voltage and current waveforms of the stack and through the rectifier. From the current waveforms the moment of inversion can be observed where it peaks to 3A. The wider 0.5A peak is when the element is conducting through the rectifier to the storage capacitor. The voltage asymptotically approaches 60V, which is also the maximum reverse bias, showing excellent agreement with equation (4). Here the moment of inversion is signified by the sharp changes from positive to negative and vice versa.

Table 2: Simulation parameters

Stack short circuit stiffness k_p	$4.26 \cdot 10^7$ N/m
Stack capacitance C_p	$8.38 \cdot 10^{-5}$ F
Electromechanical coupling θ	36.7 N/V
Load resistance R	471 Ω
Inductor quality Q_i	100 -
Inductance L	$43.3 \cdot 10^{-3}$ H
Storage capacitance C_s	$8.3 \cdot 10^{-3}$ F
Blade moment of inertia J	2387 kgm^2
Equivalent hinge stiffness k_{eq}	$1.44 \cdot 10^3$ N/rad
Blade moment amplitude M_0	$10.7 \cdot 10^3$ Nm
Piston weight M	1 kg
Lag damper radial mounting distance r	0.254 m
Rotor speed Ω	4.18 Hz
Stack section area A	$1.5 \cdot 10^{-4}$ m^2
Layer thickness t_l	$6 \cdot 10^{-5}$ m
Stack length L_s	0.25 m

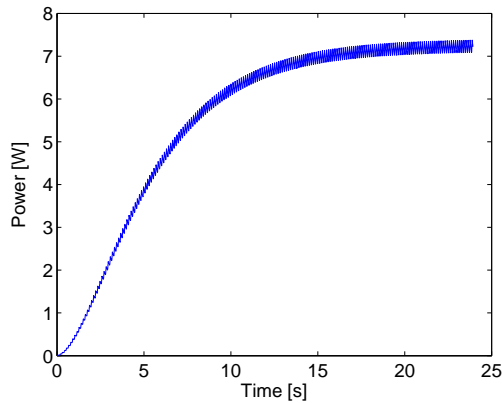


Figure 8: Power output over time

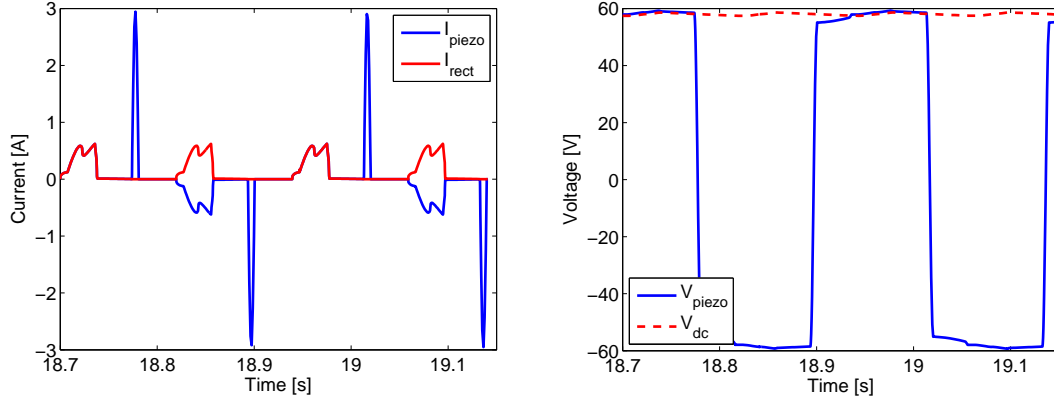


Figure 9: Resulting piezo and rectifier current (left) and piezo and DC voltage (right)

Figure 10 shows results from a parameter study where the layer thickness and inversion time are varied. Note that for these results all electromechanical variables and the layer thickness differ from those given in Table 2. As determined in the previous section too quick inversion indeed leads to a reduced amount of harvested power. The minimum harvested power is around 5W, showing that quick inversion causes nearly a 30% reduction in efficiency.

On the other hand thicker layers lead to infeasible systems due to the very large inductor required to achieve the desired voltage inversion time. This limitation is more of a practical sense and is simply presented here as a design consideration. An inductance limit of 50mH is imposed in these simulations. With no limitation all results would show the same trend, from 5W for short inversion to 7.3W for long inversion times. Taking Figure 3 into account the maximum allowed inversion time is 0.07s.

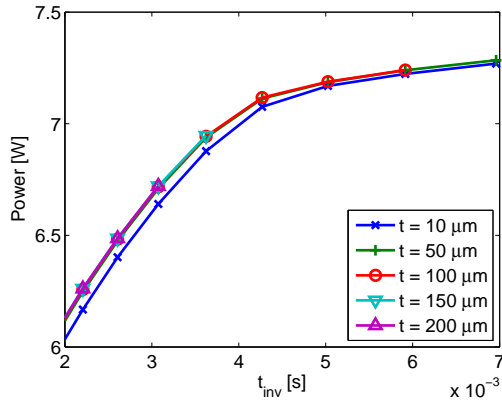


Figure 10: Power output vs voltage inversion time t_{inv} for various layer thicknesses t_l

4 DISCUSSION

Simulations show the lag damper power harvester will yield 7.3W of power. The limitation to this result is that non-linear effects (Yang et.al., 2008) and temperature effects are not included. The first will result in a reduction in harvested power due to larger losses during voltage inversion. The increasing capacitance leads to more charge stored in the capacitance C_p which must be transferred during inversion. More charge implies higher currents and larger resistive losses. It is expected that the loss may be limited by increasing the load resistance.

Increasing ambient temperature decreases the maximum reverse bias, thereby decreasing the power output, with the Curie temperature representing the limit where no power is harvested. The system must be designed to withstand temperatures from -40 to 70°C, making the upper temperature the limiting factor. Data from PICeramic indicates roughly a 20% decrease in the maximum reverse bias at 70°C and therefore a 35% decrease in power (assuming $P = V^2 / R$).

Considering the capacitance increase and temperature requirements the output is estimated to reduce to 4-5W.

The stack used here is quite large and in combination with the long inversion time the required inductance becomes quite large, forming a practical limit. The viscous losses which are incurred are proportional to the square of the velocity: \dot{u}^2 . The change in length resulting from voltage inversion also decreases and in turn the associated velocity as well if a shorter stack is used. A shorter stack or more creative solutions such as dividing the stack in two segments and inverting the voltage sequentially will quickly alleviate this problem altogether.

Health monitoring systems require a small amount of power. For instance (Olson et al., 2008) present a strain gauge which consumes only 14 μ W of power to perform strain measurements. Also, 'Microstrain' brand wireless strain and 2-axis acceleration measuring systems consume 0.1-0.5mW and 1mW respectively. Short range wireless transmission requires in the order of 100mW peak power. Fibre optic measurement systems currently consume in the order of 20W of power, however manufacturers are striving to reduce the power consumption. In the future the amount of harvested power may lie within the requirements of FO measuring systems. A single optical fibre is capable of transmitting 16 strain signals per fibre @2.5kHz measuring frequency (Smart Fibre - Smart Scan measurement system) where resistive strain gauges require two wires each, greatly simplifying the infrastructure.

Health monitoring systems in a helicopter rotor blade will greatly extend blade life. Currently the blade life is determined based on a worst case scenario. This scenario is rarely achieved in flight and the blades are discarded long before they are truly at the end of their technical life-span. Monitoring blade loads continuously will significantly increase life span and reduce running costs of rotorcraft.

The flight characteristics of the aircraft must also be preserved. With the lag damper presenting a critical component the harvester may not influence its operation. First, the force exerted by the lag damper must not change. With the voltage inversion an impulse may be developed. Figure 11 shows that for the optimized SSHI circuit this force variation is 2.3% of the peak force which is minimal but no simulations have been performed with respect to stability changes in the aircraft. Since the amount of dissipated power is higher than the lag damper alone it is not cause for major concern.

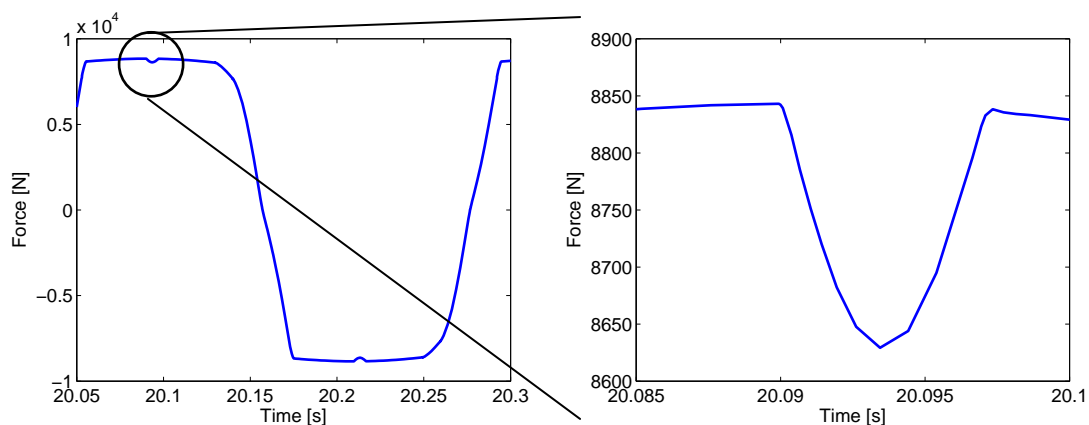


Figure 11: Developed damper force with optimized SSHI circuit

Lastly the harvester must not jeopardize the safety of the rotor craft if the system fails. Failure of the electronics does not cause any mechanical problems. On the other hand, failure of the piezo material may cause problems. These can be minimized by ensuring that the piezo material fits loosely but snugly in the rod of the damper. If the material should then fail it may still provide support for the lag damper.

Other flight conditions have not yet been considered. Considering Figure 3 it may be assumed that for slower flight speeds the amount of harvested power will be very similar until the reduced flight speed causes the peak damper velocity to decrease below 0.02m/s.

5 CONCLUSIONS

A power harvesting system for the rotor of a helicopter is presented and simulated. The simulation shows that up to 7.3W of power can be harvested from a single lag damper during horizontal flight. This is sufficient to power countless measurement nodes in the blade. The simulation does not take two important non-linear effects into account although their effect is discussed qualitatively. Including these two effects will lead to an expected output of 4-5W. If the health monitoring system in the blade requires less energy the length of the stack can be decreased to match.

Also some new design issues with respect to the SSHI circuit have been explored when it is used in a strongly coupled system. The natural frequency of the voltage inversion must be solved using the coupled electromechanical equations of motion and the influence of high mechanical damping is discussed as well.

The system is expected to have minimal influence on the dynamic stability of the helicopter and the mechanics of the lag damper. In case of failure of the harvesting system the safety of the aircraft is not compromised.

6 ACKNOWLEDGEMENTS

This project is funded by the Clean Sky Joint Technology Initiative (grant number [CSJU-GAM-GRC-2008-0019]) - GRC1 Innovative Rotor Blades, which is part of the European Union's 7th Framework Program (FP7/2007-2013). The authors are also grateful towards Augusta Westland helicopters for providing relevant flight and dynamics data.

REFERENCES

- Anton S. R., Sodano H.A., 2006, A Review of Power Harvesting Using Piezoelectric Materials, *Smart Materials and Structures*, 16(3), R1-R21
- Arms S. W., Townsend C. P., Churchill D. L., Galbreath J. H., Mundell S. W., 2006, Power management for energy harvesting wireless sensors, *EWSHM*
- Bramwell A. R. S., 2001, *Bramwell's Helicopter Dynamics*, Oxford, Butterworth-Heinemann
- Dicken J., Mitcheson P. D., Stoianov I., Yeatman E. M., 2009, Increased Power Output from Piezoelectric Energy Harvesters by Pre-biasing, *PowerMEMS*
- Dietl J. M., Garcia E., 2010, Beam shape optimization for power harvesting, *Journal of Intelligent Material Systems and Structures*, 21, 633-646
- Dogan A., Fernandez J. F., Uchino K., Newnham R. E., 1996, The "cymbal" electromechanical actuator, IEEE International Symposium on Applications of Ferroelectrics
- Feenstra J., Granstorm J., Sodano H., 2008, Energy harvesting through a backpack employing a mechanically amplified piezoelectric stack, *Mechanical Systems and Signal Processing*
- Guyomar D., Badel A., Lefeuvre E., Richard C., 2005, Toward energy harvesting using active materials and conversion improvement by nonlinear processing, *IEEE Transactions on ultrasonics, ferroelectrics and frequency control*, 52(4), 584-595
- Lefeuvre E., Badel A., Richard C., Guyomar D., 2005, Piezoelectric Energy Harvesting Device Optimization by Synchronous Charge Extraction, *Journal of Intelligent Material Systems and Structures*, 865-876
- Lefeuvre E., Badel A., Richard C., Petit L., Guyomar D., 2006, A Comparison Between Several Vibration-powered Piezoelectric Generators for Standalone Systems, *Sensors and actuators A: Physical*, 126, 405-416
- Maybury W., D'Andrea A., Hilditch R., Beaumier P., Garcia-Duffy C., 2009, *Baseline blade definition for GRC1.1*, Augusta Westland helicopters, CS JU/ITD GRC/RP/1.1/31002
- Olson S. P., Castracane J., Spoor R. E., 2008, Piezoresistive Strain Gauges for use in Wireless Component Monitoring Systems, *SAS*
- Sari I., Balkan T., Kulah H., 2007, A Wideband Electromagnetic Micro Power Generator for Wireless Microsystems, *Transducers and Eurosensors '07*
- Shen H., Qiu J., Ji H., Zhu K., Balsi M., Giorgio I., Dell'Isola F., 2010, A Low-power Circuit for Piezoelectric Vibration Control by Synchronized Switching on Voltage Sources, *Sensors and actuators A: Physical*, 161, 245-255

- Shu Y. C., Lien I. C., 2006, Efficiency of energy conversion for a piezoelectric power harvesting system, *Journal of micromechanics and microengineering*, 16, 2429-2438
- Shu Y. C., Lien I. C., Wu W. J., 2007, An improved analysis of the SSHI interface in piezoelectric energy harvesting, *Smart Materials and Structures*, 16, 2253-2264
- Wickenheiser A. M., Garcia E., 2010, Broadband vibration-based energy harvesting improvement through frequency up-conversion by magnetic excitation, *Smart Materials and Structures* (5), 19, 65020-65030
- Yang G., Yue Z., Ji Y., Li L., 2008, Dielectric nonlinearity of stack piezoelectric actuator under the combined uniaxial mechanical and electric loads, *Journal of applied physics*, 104, 074116 - 074116-6
- Zheng B. Chang C.-J., Gea H. C., 2009, Topology Optimization of Energy Harvesting Devices Using Piezoelectric Materials, *Structural and Multidisciplinary Optimization*, 38, 17-23